Enhancing Cas9 Activity in Heterochromatin

René Daer[1], Cassandra Barrett[1], and Karmella Haynes[1*]

[1]Arizona State University, School of Biological and Health Systems Engineering, 501 E. Tyler Mall, ECG 344A, Tempe, AZ, USA

[*]Corresponding author: karmella.haynes@asu.edu

Abstract

Recently, we demonstrated that closed, silenced chromatin impedes CRISPR/Cas9 editing by reducing the accessibility of DNA to Cas9/sgRNA binding at a chromosomal *Tk-luciferase* transgene. Our investigation of the underlying mechanism showed that disruption of chromatin through knock-down of the Polycomb complex enhanced Cas9-mediated editing but that over expression of the gene at the target site impeded Cas9 activity. Thus, further research is needed to establish chromatin manipulation as a practical tool for gene editing. Here, we compared two general methods for inducing an open, non-silenced state to enhance Cas9 efficiency: chromatin-disrupting inhibitor drugs and transient expression of site-specific chromatin-modifying proteins. We explored the mechanism of enhanced editing at artificially opened chromatin in HEK293 cells using deep sequencing of edited DNA and chromatin immunoprecipitation (ChIP) of histone modifications. In both cases, we observed loss of the silencing mark histone 3 lysine 27 trimethylation (H3K27me3), while only treatment with the site-specific, fusion transcriptional activator Gal4-p65 resulted in an increase in target gene expression. Our results reaffirm the previous observation that Gal4-p65-induced over-expression impedes Cas9 activity. We show that a recovery period of 9 days after Gal4-p65 expression generates a more Cas9-permissive state. Cas9 activity was fully restored following local modification of chromatin with transiently expressed Gal4-p65 at a site near the promoter and no enhancement with the small molecule chromatin inhibitor UNC1999. These results, based on ectopic chromatin at a chromosomal transgene, implicate activator-mediated chromatin remodeling as an effective method to enhance Cas9 editing at closed chromatin.

Keywords CRISPR/Cas9, chromatin

1 Introduction

CRISPR/Cas9, a nucleic acid modifying system derived from prokaryotes, is a popular tool for rapid, high-throughput genome engineering.[1,2] However, recent work has shown that chromatin, the RNA-DNA-protein complex that controls chromosomal organization and gene expression in mammalian nuclei,[3–5] inhibits Cas9 binding and nuclease activity *in vitro*[6–8] and in mammalian cells.[9,10] While Cas9 gene editing efforts have been successful in many cases, the complex structure of chromatin and its variation in different cells still pose a barrier to reliable and consistent use.

A rapidly growing body of work has determined that chromatin states have a strong influence on the accessibility of DNA to Cas9, guide RNA complexes (Cas9/gRNA), and Cas9 editing efficiency. In a series of *in vitro* studies, Hinz et al., Isaac et al., and Horlbeck et al. used reconstituted nucleosomes complexed with synthetic DNA to demonstrate that Cas9-mediated binding and cleaving of nucleosome-bound DNA is completely blocked.[6–8] It is important to note here that this synthetic sequence associates more tightly with nucleosomes than natural sequences.[11,12] Utilizing transgenic cell lines, we and others showed that ectopic constitutive HP1-mediated[9] and facultative Polycomb-mediated[10] heterochromatin compaction inhibit, and in some cases completely block, Cas9 binding and editing in HEK293T cells and HEK293 cells, respectively. Notably, editing at three sites in the same region was not reduced by heterochromatin, suggesting that inhibition of Cas9 can be discontinuous across regions of closed chromatin.[10] Research so far suggests that disruption of closed chromatin might support a Cas9-permissive state. To achieve control over Cas9-mediated editing in heterochromatin, further investigation of the relationship between chromatin states, gene expression, and Cas9 editing in cells is needed.

To this end, we investigated methods for improving Cas9 editing by artificially opening chromatin previously inhibited by Polycomb-mediated heterochromatin (Figure 1A). Polycomb group (PcG) proteins are critical for controlling gene expression in stem cell maintenance and differentiation by depositing and maintaining the silencing mark histone 3 lysine 27 trimethylation (H3K27me3).[17,18] They are also responsible for silencing oncogenes; hyperactive PcG proteins are observed in many cancers.[19–22] Polycomb-regulated genes are distributed over thousands of sites along chromosome arms in gene-rich regions. Therefore, Polycomb complexes represent a significant barrier to genome editing. In our previous work, we demonstrated that artificial conversion of closed chromatin via siRNA-mediated knockdown of the repressive Polycomb protein Suz12 was accompanied by an increase in Cas9-mediated editing efficiency.[10] However, it is difficult to control the consistency and magnitude of siRNA delivery. Therefore, we set out to explore alternative methods to induce an open, Cas9-accessible state at sites of previously silenced chromatin.

Here, we expanded our investigation to two methods for dis-

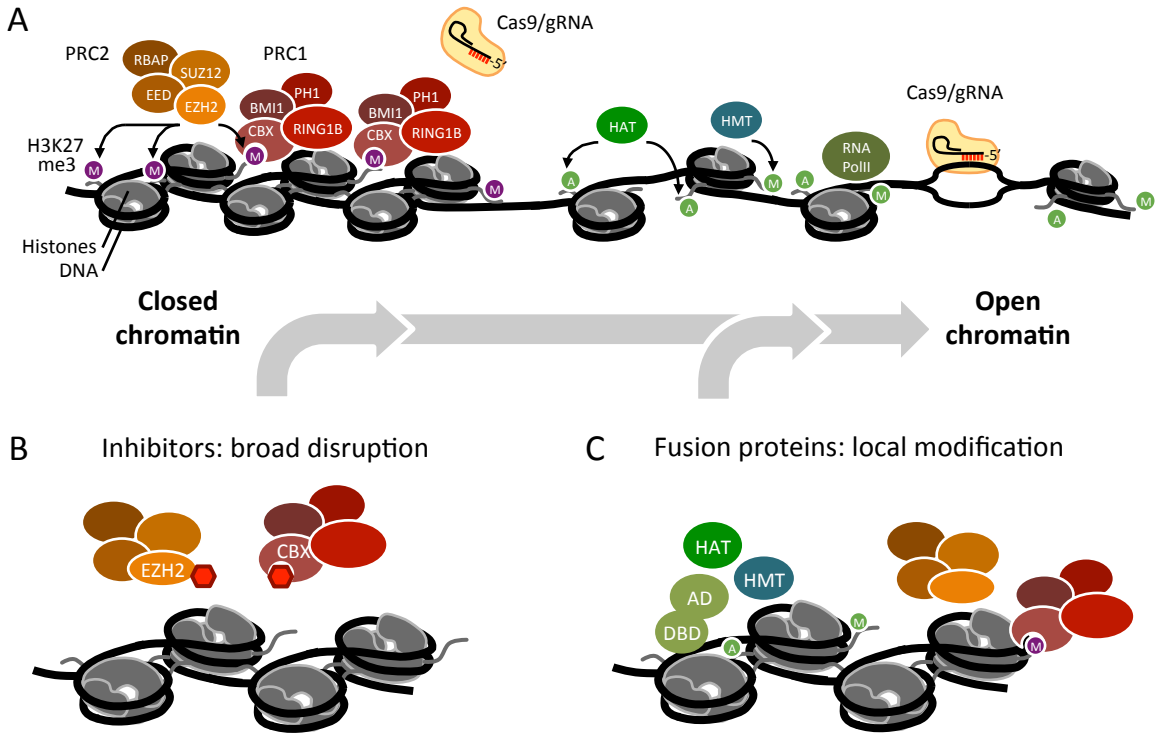

Figure 1: Research of Cas9 activity in chromatin suggests that facultative heterochromatin inhibits Cas9 editing while open chromatin is permissive to Cas9. (A) The PRC2 (Polycomb repressive complex 2) holoenzyme generates the silencing chromatin mark histone 3 lysine 27 trimethylation (H3K27me3) (purple M). PRC2 includes Suppressor of Zeste 12 (SUZ12), Embryonic ectoderm development (EED), Retinoblastoma-binding protein (RbAp), and Enhancer of zeste 2 (EZH2).[3,5] The PRC1 (Polycomb repressive complex 1) (PRC1) interacts with PRC2 to propagate the silencing mark. PRC1 includes Chromobox protein homolog (CBX), Ring finger protein 1b (RING1B), and Polycomb group RING finger protein 4 (BMI1).[3,5] Polycomb proteins support histone compaction and block access of DNA to RNA polymerase and Cas9.[9,10] Chromatin remodelers (not shown), histone acetyltransferases (HATs), and histone methyltransferases (HMTs) generate modifications that support open chromatin, accessible DNA, and a transcriptionally permissive state.[13,14] (B) Inhibitors (red hexagons) of chromatin-silencing proteins disrupt closed chromatin in a global, non-specific manner[15] (C) Synthetic fusion proteins containing a DNA binding domain (DBD) and activating domain (AD) can be used to recruit chromatin-remodeling proteins to a specific locus.[16]

rupting closed chromatin: a PcG-inhibiting drug (Figure 1B) and site-directed chromatin modification with a targeted transcriptional activator fusion protein (Figure 1C). Transcription-activating fusion proteins have been shown to change chromatin accessibility.[16] Furthermore, Isaac et al. and Horlbeck et al. used nucleosome-sliding enzymes to improve Cas9 cleavage of DNA complexed with nucleosomes *in vitro*.[7,8] Together, these studies suggest that targeting silenced chromatin for remodeling could improve Cas9 editing in human cells. To test this hypothesis, we determined changes in transgene expression and histone marks following chromatin modification. We next determined the effect of global and targeted chromatin reopening approaches on Cas9 efficiency. We found that strong induction of transcription from a nearby promoter followed by culturing for several days to allow recovery of a generally permissive chromatin state restored full Cas9 activity at a target site downstream of the promoter. Our results inform a general approach for overcoming challenges associated with site-specific Cas9 inaccessibility.

2 Results

2.1 Depletion of H3K27me3 via UNC1999 is not Sufficient to Generate an Expression-Permissive State

We hypothesized that treatment with with a broad acting, PcG-inhibiting drug would disrupt closed chromatin and allow for Cas9 to bind and edit a previously blocked target site (Figure 1B). UNC1999 is a small molecule drug that disrupts heterochromatin in mammalian cells by binding to the active site of the methyltransferase Enhancer of zeste 2 (EZH2) to prevent the methylation at H3K27me3, a modification that supports Polycomb complex formation and a closed chromatin state.[15] Konze et al. showed that UNC1999 completed depleted H3K27me3 from the epigenome by directly inhibiting EZH2 and EZH1 in both MCF7 (a human breast cancer cell line) and HEK293T cells.[15] They also reported that UNC1999 is effective when fed to and injected into mice with no observed toxicity.[15] This result suggests that UNC1999 is potentially a minimally toxic option for chromatin disruption in mammalian cells. UNC1999 can be diluted in media and therefore can

be delivered to all cells in a culture, making it an attractive option for difficult to transfect cell lines.

We used a transgenic cell line, referred to here as Gal4EED/luc, in which we can induce Polycomb-mediated heterochromatin at a *luciferase* transgene.[10,23] After treatment with doxycycline (dox), the cells express a Gal4-embryonic ectoderm development (EED) fusion protein which binds to a Gal4 enhancer sequence (UAS) upstream of a *luciferase* transgene. Gal4EED recruits PcG proteins, resulting in accumulation of the H3K27me3 silencing mark and *luciferase* silencing. The Luc14 cell line does not contain the Gal4EED fusion protein construct and is used here as an open chromatin control (the absence of the silencing mark H3K27me3 was confirmed previously in Daer et al.). The *luciferase* transgene was genomically inserted with random integration Hansen et al. Based on series of PCR's with overlapping amplicons that spanned the transgene, we estimated that the breakpoint for transgene linearization and integration occurred at 2050 bp to 2457 bp upstream of the nucleation site (Gal4 UAS) (Figure S1).

First, we determined the impact of UNC1999 on the expression and chromatin states of the *luciferase* transgene. We silenced the chromatin at *luciferase* by adding dox for 96 h. At 120 h (24 h after dox removal), we added 10 µM of UNC1999 for 120 h (see Table S1 for kill curve results). At 264 h (24 h after UNC1999 removal), we measured Luciferase activity and performed chromatin immunoprecipitation assay followed by quantitative PCR (ChIP-qPCR) to determine H3K27me3 occupancy. While UNC1999 did not significantly increase Luciferase activity (Figure 2A), we saw a significant decrease in H3K27me3 compared to the DMSO control ($p < 0.01$) (Figure 2B). We conclude that at 10 µM, UNC1999 can effectively remove the silencing mark H3K27me3 from the silenced transgene but does not initiate transcriptional activation under the conditions tested here. This is consistent with previous work demonstrating that removal of the H3K27me3 silencing mark alone does not induce gene expression in embryonic stem cells[24] and that DNA methylation and complete transcriptional silencing of cancer genes persist after depletion of EZH2.[25] We next investigated whether this removal of the silencing mark is sufficient to improve Cas9 editing.

2.2 UNC1999 Treatment Does Not Improve Cas9 Editing

To determine whether UNC1999 treatment of closed chromatin could be used to restore Cas9-mediated editing to levels observed in open chromatin, we compared Cas9 activity after the same treatments we used for the expression and ChIP-qPCR. Briefly, cells were silenced with dox and then treated with either vehicle control DMSO or UNC1999 (Figure 3A). At 24 h post DMSO or UNC1999 removal, we transfected with Cas9/sgRNA expressing plasmids with sgRNAs targeting sg046, 32, 25, and 48 (Figure 3B). Sg046, 32, and 48 were chosen to represent sites where Cas9 activity is inhibited by closed chromatin.[10] These sites also represent varying distances from the heterochromatin nucleation site upstream of the transcription start site. Sg046 and 32 are proximal to the Gal4 UAS sequence (within 300 bp) while sg048 is distal (>1000 bp downstream of the TSS). Sg025 is a target site that showed no change in editing efficiency within closed chromatin[10] and was therefore included in the studies reported here as a control. Their sequences are listed in Supplementary Table S3. At 72 h post transfection, we collected the treated cells and assayed for Cas9 editing using deep sequencing to quantify the proportions of insertion and deletion (INDEL) variants generated by non-homologous end-joining (NHEJ). We observed that mean editing was reduced at sg046, sg032, and sg048 in closed chromatin, DMSO-treated cells compared to the open chromatin control (sg046 $p < 0.001$, sg032 and sg046 $p < 0.005$) (Figure 3B). UNC1999 treatment did not restore Cas9 editing at any of the 4 target sites tested. Furthermore, at two target sites, treatment with UNC1999 showed an even greater inhibition than in the vehicle control (sg046 $p < 0.001$ and sg025 $p < 0.01$). The position of the most frequently edited sites (the nucleotide immediately adjacent the predicted cut site) was the same under all conditions (Figure 3C), suggesting that treatment with UNC1999 did not alter the pattern of editing in general. We conclude that UNC1999 treatment under these conditions is not effective in improving Cas9-mediated editing at sites in heterochromatin.

2.3 Gal4-p65 Activates Transcription and Modifies Chromatin at a Previously Silenced Locus

Our previous work demonstrated that a fusion transcriptional activator composed of the Gal4 DNA binding domain and the p65 protein (NF-kB) can activate gene expression at a PcG-silenced *luciferase* gene.[10] P65 is known to interact with several transcriptional activators including BCL3, JUN, NFKB1, NFKBIA, and NFKBIB.[26] It also directly interacts with CREBBP, which acetylates H3K27, directly counteracting PcG methylation at H32K27. In addition, SETD7 directly regulates p65 promoter binding and nuclear localization, while also adding the activation-associated histone 3 lysine 4 trimethylation mark (H3K4me3).[27] Here, we tested whether the transcription-activating fusion protein Gal4-p65 induces sustained transcriptional activation and chromatin remodeling at the PcG-silenced *luciferase* transgene. We measured the change in *luciferase* expression, the silencing-associated H3K27me3 mark, and the activation-associated H3K4me3 mark 9 days after treatment with the Gal4-p65 activator.

We induced silencing at *luciferase* in GAL4EED cells as in previous experiments by treating the cells with dox for 96 h. At 24 h after dox removal, we transfected with the Gal4-p65 expressing plasmid. After 72 h and 216 h (9 days), we collected the cells and assayed for Luciferase activity. We performed ChIP-qPCR on samples collected after 9 days and measured for H3K27me3 and H3K4me3 enrichment using qPCR.

We detected strong and sustained re-activation of *luciferase* at 3 days and 9 days following transfection with Gal4-p65-expressing plasmids (Figure 4A). This is consistent with our previously reported results.[10]

Using ChIP-qPCR, we determined the change in H3K27me3 after treatment with the Gal4-p65 activator. Similar to treatment with UNC1999, we saw a significant reduction in the amount of H3K27me3 9 days post transfection with the Gal4-p65 expressing plasmid ($p < 0.005$) (Figure 4B). This suggests that Gal4-p65 is either recruiting chromatin remodelers that

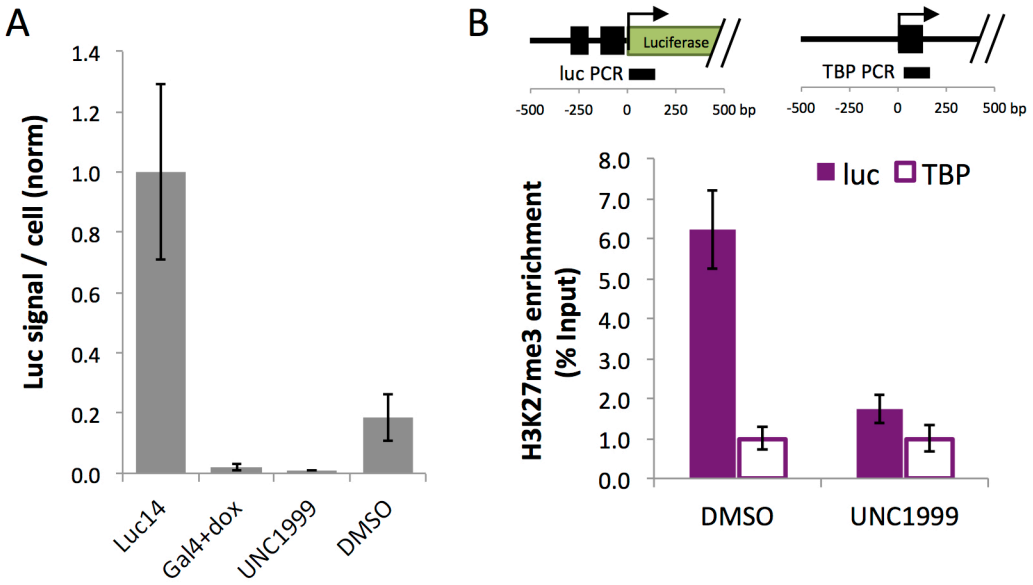

Figure 2: UNC1999 depletes histone 3 lysine 27 trimethylation (H3K27me3). (A) *Luciferase* expression in UNC1999-treated cells was near or below *luciferase* levels in untreated cells (Gal4+dox) and cells treated with the vehicle control (DMSO). Error bars indicate standard deviation of $n = 3$ biological replicates. (B) Chromatin immunoprecipitation assay followed by quantitative PCR (ChIP-qPCR) showed significant reduction in H3K27me3 enrichment at *luciferase* after treatment with UNC1999 compared to the vehicle control ($p < 0.01$). A constitutively active control locus, TATA-binding protein (TBP), was used as a negative control for ChIP-enrichment of H3K27me3. Error bars indicate standard deviation of $n = 3$ replicate pulldowns from a single chromatin prep.

are removing the nucleosomes or the silencing mark, or that strong recruitment of RNA polymerase is responsible for the change in chromatin.

To determine whether p65 localization results in addition of active chromatin modifications, we tested for the presence of an activating mark, H3K4me3. We saw some reduction in the mark between active and silenced though it was not significant ($p = 0.06$) (Figure 4B). We did observe a significant increase in the active mark between the silenced state and the reopened state ($p < 0.01$).

Interestingly, our data indicate that the active and silenced state both have the H3K4me3 mark (Figure 4B). This mark is associated with bivalent promoters and is often seen together with H3K27me3.[28] This suggests that recruitment of PRC1 and PRC2 does not result in removal of H3K4me3 at this site.

2.4 Gal4-p65 pre-treatment improves Cas9 Editing at a previously silenced locus

Gal4-p65-induced activation of *luciferase* and the accompanying changes in chromatin structure (Figure 4B) led us to hypothesize that local chromatin remodeling via Gal4-p65 would enhance Cas9-mediated editing at a site that was previously blocked by heterochromatin, as illustrated in Figure 1C. In previous work we tested this idea in *luciferase*-silenced HEK293 cells that were co-transfected with a Gal4-p65-expressing plasmid and Cas9/gRNA-expressing plasmids.[10] *Luciferase* became activated, suggesting a transcriptionally permissive state, but editing efficiency was not significantly higher than editing at PcG-repressed *luciferase*. Furthermore, we observed a decrease in editing efficiency at a non-repressed site that was hyper-activated by Gal4-p65. Competition between Gal4-p65 (and interacting proteins) and Cas9/gRNA might contribute to the observed reduction in Cas9 activity. In order to reconcile p65's role in promoting an open chromatin state with the observed blocking of Cas9's access to DNA, we asked whether transient Gal4-p65 expression followed by a recovery period to allow for depletion of Gal4-p65 would generate a Cas9-permissive chromatin state.

Having established that transcriptional activation and activation-associated histone modifications were sustained nine days post-treatment with Gal4-p65 (Figure 4), we compared Cas9-mediated editing efficiencies at four target sites (Figure 5A). We transfected with either the Gal4-p65 plasmid and the Cas9/sgRNA plasmid (for co-treatment) or the Gal4-p65 plasmid alone (for pre-treatment), then with Cas9/gRNA 9 days later (2 passages). Cas9 editing was allowed to occur at 37 °C for 72 h before genomic DNA was prepared from each sample. In pre-treated cells, the total recovery period following Gal4-p65 over expression was 9 days at the time of the genomic DNA prep. We tested four sgRNA target sites: sg046, 32, 25, and 48 (Figure 5B). Active and Silenced controls in Figure 5B and C are the same data presented in Figure 3.

Mean editing efficiencies in Gal4-p65 co-treated cells at all four target sites generally agreed with our previous experiments in which we tested just one site (sg034, located between sg032 and sg025) in the same 1.1 kb region downstream of the PcG nucleation site.[10] We saw no recovery of Cas9 editing efficiency in the co-treated cells (Figure 5B, Closed +Gal4p65). Editing efficiency values were at or below closed chromatin levels for sg032, 25, and 48 or sg046, respectively. The the most frequent INDELs showed no obvious change in position relative the predicted cut sites (Figure 5C). Therefore our results do not demonstrate any change in Cas9 specificity and

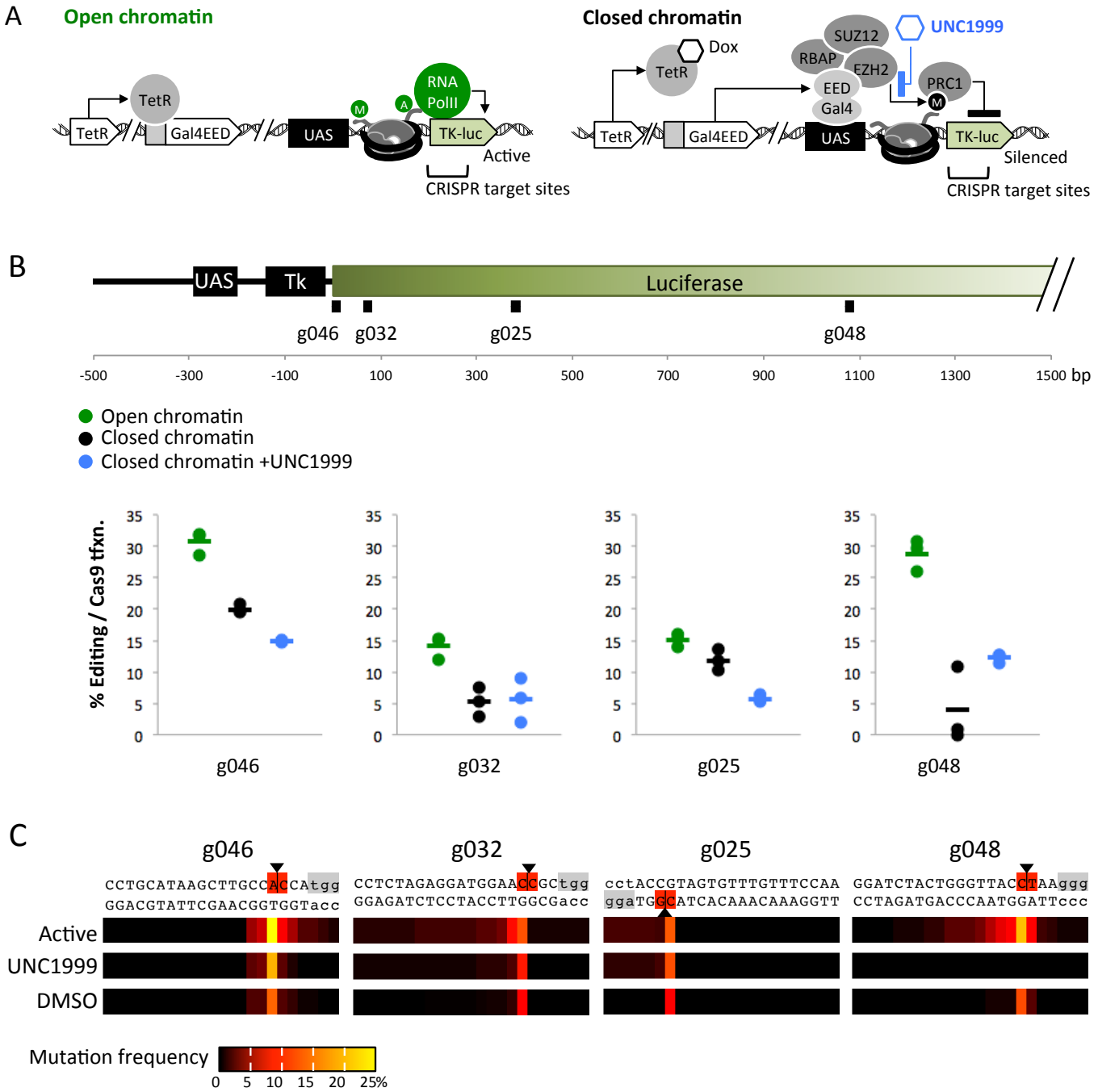

Figure 3: UNC1999 effect on Cas9 editing. (A) Summary of approach. Open chromatin is characterized by transcription of the *luciferase* transgene (Figure 2A) and absence of the silencing mark H3K27me3.[10] Closed chromatin is induced after addition of doxycycline (dox) and is characterized by reduced *luciferase* expression (Figure 2A) and accumulation of the silencing mark histone 3 lysine 27 trimethylation (H3K27me3) (Figure 2B and Daer et al.). Treatment with UNC1999 (blue hexagon) inhibits the Enhancer of zeste 2 (EZH2) subunit of Polycomb Repressive Complex 2 (PRC2), resulting in removal of the silencing mark H3K27me3 (Figure 2B and Konze et al.). (B) Map of the *luciferase* transgene and the sgRNA target sites. Comparison of Cas9 editing efficiencies at each sgRNA target site for three different chromatin states. "Open chromatin" (green) are untreated Luc14 cells transfected with Cas9/sgRNA expressing plasmids with sgRNAs targeting sg046, 32, 25, and 48. "Closed chromatin" (black) and "Closed chromatin +UNC1999" (blue) are Gal4EED/luc+dox silenced cells treated with either vehicle control (DMSO) or UNC1999. At 24 h post doxycycline (dox) removal, cells were treated with DMSO or UNC1999 for 72 h. At 24 h post DMSO or UNC1999 removal, cells were transfected with Cas9/sgRNA expressing plasmids with sgRNAs targeting sg046, 32, 25, and 48. For all samples, editing efficiencies were measured 72 h post transfection with Cas9/sgRNA plasmids. Bars indicate the mean of three biological replicates (dots). (C) DNA heat maps indicate the frequency at which each base position was affected by an insertion or deletion (INDEL).

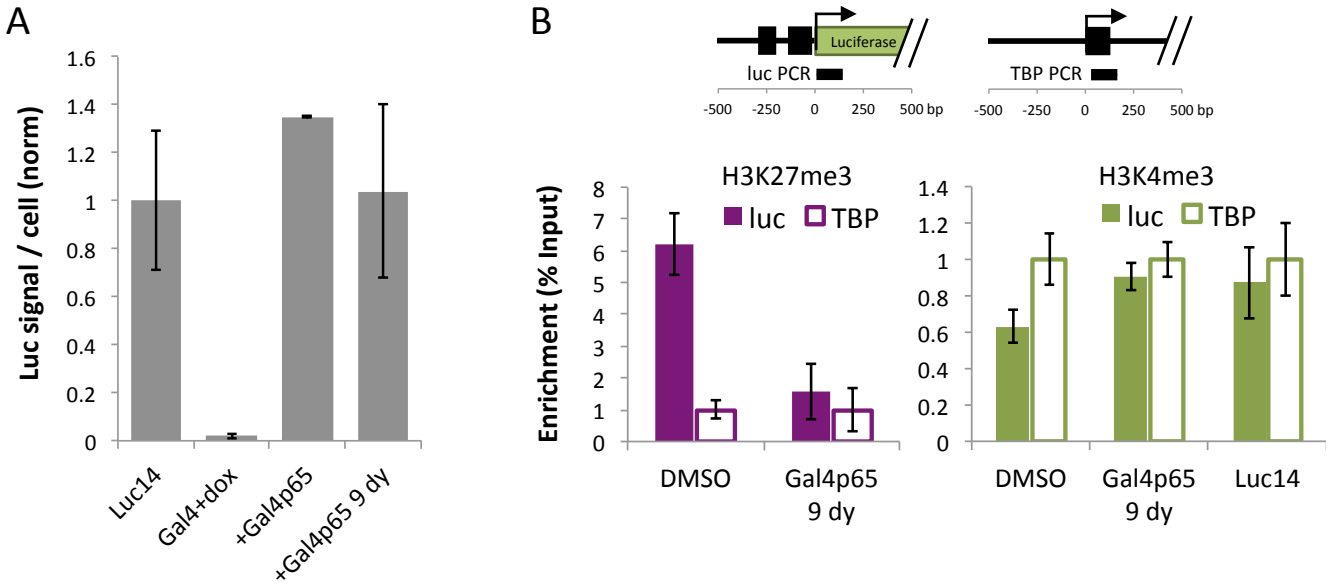

Figure 4: Targeted transcriptional activator Gal4-p65 increases *luciferase* expression and modifies local chromatin. GAL4EED cells were treated with doxycycline (dox) for 96 h and transfected with the Gal4-p65 expressing plasmid. (A) Gal4-p65 increases gene expression at the previously silenced *luciferase* transgene. Luciferase activity was measured after 72 h or 216 h (9 days). Error bars indicate standard deviation of $n = 3$ biological replicates. (B) Gal4-p65 reduces H3K27me3 at the *luciferase* transgene. H3K4me3 is present in each chromatin state but increased after treatment with Gal4-p65. Error bars indicate standard deviation of $n = 3$ replicate pulldowns from a single chromatin prep.

NHEJ products within the sequenced regions. Our results suggest that Gal4-p65 accumulation and activator recruitment inhibits Cas9 activity by blocking access of Cas9/gRNA to the target sites.

At each sgRNA target site, we compared editing efficiencies of Cas9 in cells pre-treated with Gal4-p65 with co-treated cells and the silenced DMSO control (Figure 5B and C). As expected, we did not observe any significant differences in editing efficiency at the control target site sg025. At one of the proximal sites (sg032) and the distal site (sg048), the mean editing efficiency approached full recovery (open chromatin levels). The most significant enhancement of editing was observed at the distal site sg048 ($p < 0.005$, Closed +Gal4p65, 9 day recovery versus closed chromatin). The target site closest to the heterochromatin nucleation site and the TSS, sg046, showed no significant increase in editing compared to the closed chromatin control. Editing was significantly higher than in the Gal4p65 co-treated cells ($p < 0.01$), suggesting that the site was initially blocked during Gal4p65 over-expression, but did not take on a Cas9-permissive state after recovery. Overall, these results suggest that initial, transient over-expression of a targeted transcriptional activator is followed by gradual remodeling of chromatin into a state that enables Cas9-mediated editing (Figure 5).

3 Discussion

Here, we investigated methods for improving Cas9 editing at sites located in silenced chromatin. First we tested how artificial opening of closed chromatin changes gene expression and local chromatin. We next looked at how these changes effect Cas9 editing activity. We compared two approaches: indirect activation via the disruption of closed chromatin (Figure 3A) and fusion-mediated activation (Figure 5A). We targeted Cas9 to four sites along a *luciferase* transgene, three of which show inhibition by heterochromatin (sg046, 32, and 48) and one control site that does not show inhibition (sg025). We determined that removal of the silencing mark H3K27me3 by a global chromatin inhibitor drug is not sufficient to recover Cas9 editing. We confirmed that strong transcriptional activation inhibits Cas9 activity.[10] We identified pretreatment with a strong transcriptional activator remodels heterochromatin to allow for improved Cas9 access to target DNA.

We demonstrated that while UNC1999 effectively removed H3K27me3 from the *Tk-luciferase* transgene (Figure 2B), it was not sufficient to induce gene activation (Figure 2A) or enhance Cas9 editing at the sites tested (Figure 3B and C). Our results support previous observations that removal of H3K27me3 does not result in local gene activation[24] or remodeling of chromatin to an open state; additional silencing marks can remain after inhibition of Polycomb proteins and maintain gene silencing.[25] We conclude that incompletely activated chromatin is not sufficient to improve DNA accessibility to Cas9 editing (Figure 3B and C).

Broad acting chromatin remodelers such as UNC1999 provide several potential advantages over fusion protein-dependent approaches. Researchers can manipulate chromatin at many sites at once, allowing for multiplex targeting of difficult sites. Furthermore, there are target sites in which gene activation may not be desirable, such as master transcriptional regulators or oncogenes. Finally, low molecular weight compounds do not require transfection, are easier to deliver, and can affect sites at which DNA-binding modules cannot be designed (e.g., low com-

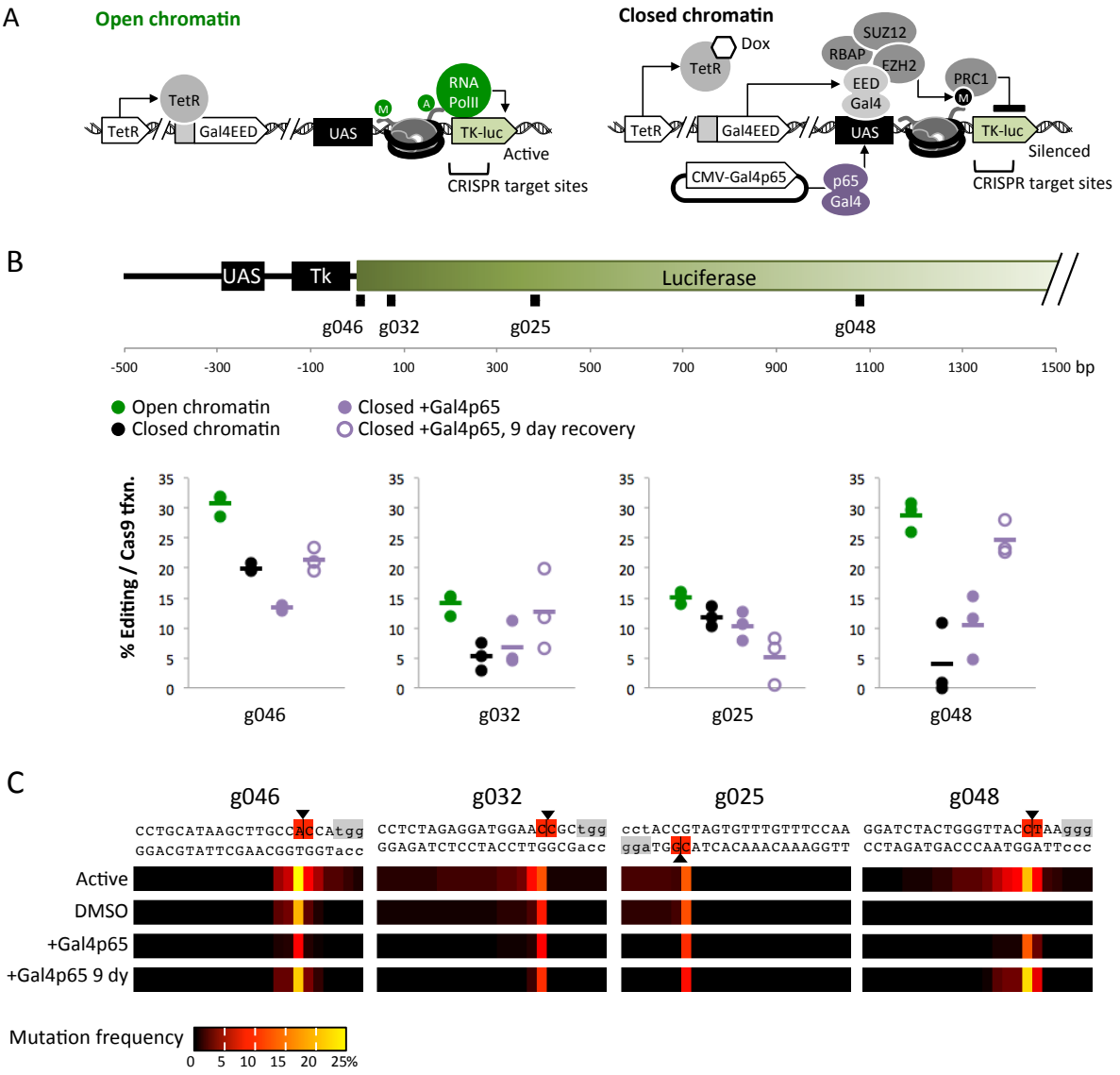

Figure 5: Pre-treatment with transcriptional activator improves Cas9 editing at closed chromatin while co-treatment does not. (A) Summary of approach. Open chromatin allows transcription of the *luciferase* transgene (Figure 4A) and does not have the silencing mark H3K27me3.[10] Closed chromatin is induced after addition of doxycycline (dox) and is characterized by reduced *luciferase* expression (Figure 4A) and accumulation of the silencing mark H3K27me3 (Figure 4B and Daer et al.). After silencing the chromatin, Gal4EED/luc cells were transfected with the CMV-Gal4p65 plasmid, which results in long-term activation of *luciferase* expression and local chromatin remodeling (Figure 4B). (B) Map of the *luciferase* transgene and the sgRNA target sites. Comparison of Cas9 editing efficiencies at each sgRNA target site for different chromatin states. "Open chromatin" (green) are untreated Luc14 cells transfected with Cas9/sgRNA expressing plasmids with sgRNAs targeting sg046, 32, 25, and 48. "Closed chromatin" (black) are Gal4EED/luc+dox silenced cells treated with DMSO vehicle control for 72 h, transfected with Cas9/sgRNA expressing plasmids with sgRNAs targeting sg046, 32, 25, and 48 at 120 hour (5 days) post dox removal. "Closed +Gal4p65" (purple filled) are Gal4EED/luc+dox silenced cells cotransfected with CMV-Gal4p65 plasmid and Cas9/sgRNA expressing plasmids with sgRNAs targeting sg046, 32, 25, and 48 at 24 h post dox removal "Closed +Gal4p65, 9 day recovery" (purple outlined) are Gal4+dox silenced cells transfected with CMV-Gal4p65 plasmid at 24 h post dox removal. Transfected cells were cultured for 216 h (9 days) and the transfected with Cas9/sgRNA expressing plasmids with sgRNAs targeting sg046, 32, 25, and 48. For all samples, editing efficiencies were measured 72 h post transfection with Cas9/sgRNA plasmids. Dots indicate individual replicates and bars indicate the average of the three biological replicates. (C) Heat maps of the mutational frequency for a representative biological replicate. Note: "Open chromatin" and "Closed chromatin" data are the same data presented in Figure 3.

plexity sequences). Future work should investigate additional chromatin inhibiting drugs and drug combinations such as histone deacetylase (HDAC) inhibitors and DNA methyltransferase (DNMT) inhibitors for their impact on Cas9 activity in heterochromatin.

We have determined specific conditions in which targeted hyper-activation can generate a Cas9-accessible state in the ectopic chromatin model system used here. Pre-treatment with the Gal4-p65 activator shows promising improvement in editing at a target site previously inhibited by PcG mediated heterochromatin (Figure 5B and C). We confirmed our previous observation that high-transcriptional activity can impede Cas9 editing possibly through steric hindrance and competition with the high occupancy of the Gal4 UAS with activator proteins and RNA PolII. Co-treatment with the Gal4-p65 activator showed no improvement in editing and, at one site, significant inhibition compared to the silenced state (Figure 5B and C). Pre-treatment with the activator caused removal of the H3K27me3 silencing mark, addition of the H3K4me3 activating mark, gene activation (Figure 4), and enhanced Cas9 editing near open-chromatin levels at target sites previously inhibited by closed chromatin (Figure 5B and C). We demonstrate that, under these conditions, pre-treatment with fusion-activators changes the local chromatin environment to allow Cas9 editing at previously blocked sites.

The key advantage of the activator Gal4-p65, or in general any DNA-binding domain with an effective transcriptional activator, is the ability to target a single genomic locus without disrupting the expression of other genes. Weaker transcriptional activators could provide additional options without the need for time delay if they remodel chromatin without creating steric competition. While the fusion protein tested in this study was targeted to a Gal4 binding sequence, it could be modified to bind endogenous sites using other customizable DNA binding modules such as dCas9/sgRNA, zinc fingers (ZF) or TAL effectors, making it potentially widely applicable.[16] We demonstrated that targeted remodeling enhances Cas9 editing >1000 bp downstream from the Gal4 binding site (UAS), suggesting that dCas9/sgRNA, ZF, or TAL effectors fusions could be targeted to an accessible locus to enhance accessibility at a distal site. In conclusion, our study lays the foundation for a strategy to enable Cas9-mediated editing in heterochromatin.

4 Methods

4.1 Cell Lines and Plasmids

For this study, we used HEK293 cells carrying a *firefly luciferase* transgene (Luc14) or the *firefly luciferase* transgene plus an inducible *tetO-Gal4EED* transgene (GAL4EED), described previously ([10,23]). Briefly, in the GAL4EED cell line, chromatin state at the *Gal4UAS-TK-luciferase* transgene can be controlled by the addition of doxycycline (dox); cells are open until treated with dox for 96 h.[10] The *Gal4UAS-TK-luciferase* transgene in the Luc14 cell line remains open as there is no *Gal4EED* transgene. These states have been characterized by Luciferase expression assays and ChIP-qPCR.[10,23]

Cas9 transfections were done using pU6-(BbsI)_CBh-Cas9-T2A-EGFP (DNASU UnSC00746685) built from pX330-U6-Chimeric_BB-CBh-hSpCas9 (a gift from Feng Zhang, Addgene plasmid #42230) (described in Daer et al.). The pU6-(BbsI)_CBh-Cas9-T2A-EGFP expresses the human optimized Cas9 protein and EGFP from the same mRNA transcript. Guide RNAs sg025, sg032, sg046, and sg048 were cloned into pU6-(BbsI)_CBh-Cas9-T2A-EGFP (described in Daer et al.). Gal4-p65 transfections were done with plasmid CMV-Gal4p65_MV1 (DNASU UnSC00746686) which expresses the Gal4-mCherry-p65 fusion protein from a CMV promoter. Sequences for each plasmid used in this study are available online with annotations (link).

4.2 Cell Culturing and Transfection

Luc14 and GAL4EED cells were cultured using Gibco DMEM high glucose 1× (Life Technologies) with 10% Tet-free Fetal Bovine Serum (FBS) (Omega Scientific), 0.5 µg/ml puromycin (puro) and 1% penicillin streptomycin (ATCC) and grown at 37 °C in a humidified 5% CO_2 incubator. To induce chromatin silencing at *luciferase* in GAL4EED cells, puro was removed and 1 µg/ml of dox (Santa Cruz Biotechnology) was added to the media for 96 h.

For transfections, cells were seeded in 12-well plates such that 24 h later they were at 90% confluency. Lipid complexes were formed using 500 ng plasmid, 3 µl Lipofectamine LTX, and 1 µl Plus Reagent (Life Technologies) per well and diluted in Gibco Opti-MEM (Thermo-Fisher) to a final volume of 100 µl per well. For all but the p65 pre-treatment assays, cells were collected for analyses 72 h post transfection.

For UNC1999 treatment, powdered UNC1999 (Cayman Chemical) was dissolved in DMSO to 10 mM. Toxicity was determined using a dilution curve (Table S1). Gal4EED cells were treated for 96 h with dox to induce silencing. After 24 h without dox, cells were treated with 10 mM UNC1999 by diluting 1 µl of 10 mM UNC1999 per 1 ml media for 72 h. Control cells were treated with 1 µl of DMSO (vehicle) per 1 ml media. Cells were grown for 1 day in media without UNC1999 before Luciferase assay (described below), transfection with Cas9/sgRNA plasmids (described above) or ChIP-qPCR (described below).

4.3 Luciferase Assays

Cells were washed with PBS and collected with 0.2 ml of trypsin-EDTA (0.25%) (Life Technologies) and 0.5 ml DMEM. Cells were pelleted at 200 g for 5 min at room temperature, washed with PBS, pelleted again, resuspended in 1 ml of FACS buffer (1% FBS in 1× PBS), and filtered with 35 µm cell strainers (Electron Microscopy Sciences). Transfection efficiencies for each sample were determined by measuring the mCherry positive cells in 10 000 live cells with the BD Accuri C6 Flow Cytometer and accompanying software (BD Biosciences). Cell counts to normalize Luciferase activity were determined by counting the number of live cells in 20 µl from each sample by flow cytometry. Luciferase assay was performed in triplicate, with 100 µl of each sample diluted in 100 µl D-luciferin diluted in buffer [Steady-Luc Firefly HTS Assay Kit (Biotium)] according to manufacturer's protocol, in CORNING and Costar 96-well Plates, white sides, clear bottom (Bioexpress). One hundred µl of FACS buffer with 100 µl of diluted D-luciferin

was used as background control. The reaction incubated for 5 min at room temperature with orbital shaking and luminescence was determined with a Synergy H1Multi-Mode Reader (Biotek). Luciferase activity normalized per cell was calculated:

$$\frac{\text{Luciferase}}{\text{cell}} = \text{Luciferase signal} - \frac{\text{background signal}}{\text{cell count in } 20\,\mu\text{l} \times \frac{100\,\mu\text{l}}{20\,\mu\text{l}}}$$

4.4 Cas9 Activity Assays

After 72 h of growth post-transfection with pU6-(BbsI)_CBh-Cas9-T2A-EGFP (DNASU UnSC00746685) with sgRNAs sg025, sg032, sg046, and sg048,[10] cells were collected as with 0.2 ml of trypsin and 0.5 ml of DMEM and spun for 5 min at 500 g at room temperature. Supernatant was discarded and cells were resuspended in 250 µl of 1× PBS. To determine transfection efficiency, 50 µl were counted by flow cytometry, gated for live cells, and the percent of GFP positive cells was recorded. Genomic DNA was extracted from the remaining 200 µl of cells using the QIAamp DNA Mini Kit (Qiagen) and eluted in 100 µl of nuclease-free water.

PCR of gDNA was performed using GoTaq 2× mastermix (Promega) using primers P198/198 (sequences listed in Supplemental Table S2) [95 °C for 10 min; 34 x (95 °C for 30 s; 58 °C for 30 s; 72 °C for 120 s)]. Nested PCR was performed by diluting 2 µl of PCR product into 500 µl of water and Phusion High-Fidelity DNA Polymerase (Thermo Scientific) (primers listed in Supplementary Table S3 and corresponding sequences in Supplementary Table S4). PCR reactions were purified using the Genelute PCR Cleanup Kit (Sigma) and submitted to the Center for Computational and Integrative Biology (CCIB) Core Facility (Massachusetts General Hospital, Cambridge, MA) according to their requirements for sequencing.

4.5 Crosslinked Chromatin Immunoprecipitation

For p65 co-treatment ChIP, Luc14s and Gal4EED + dox cells were transfected with 18 µg p65 plasmid using the 100 µl Neon transfection system (Invitrogen) following the recommended protocol (1100 V pulse voltage, 20 ms pulse width, 2 pulses, with cell density 5×10^6/ml). Cells were grown at 37 °C for 72 h, fixed as described below, and sorted using the BD FACSAria II cell sorter. Lysis and sonication steps were performed same day as described below. For chromatin remodeler treatment ChIP, Gal4EED + dox cells were transfected with 18 µg of each chromatin remodeler plasmid using the Neon transfection system as described above. For p65 pre-treatment ChIP, Gal4EED + dox cells were transfected with Lipofectamine as described above and grown at 37 °C for 9 days.

Cells were washed and collected as described above and fixed with 1% formaldehyde (Thermo Fisher Scientific) in 1× Dulbecco's PBS for 10 min. The reaction was quenched with 125 mM glycine (Sigma) for 5 min at room temperature with gentle rocking followed by four washes with 1× PBS and Pierce Protease Inhibitors (Thermo Fisher Scientific), two for 5 min at room temperature and two without incubation. Cells were pelleted between each wash at room temperature for 5 minute at 500 g. During the last wash step, 10 µl of cells were transferred to a new tube, diluted into 90 µl of 1× PBS, and 20 µl of cells were counted via flow cytometry. Total number of cells were calculated for each sample. Cells and nuclei were lysed with cell lysis buffer *( )* and nuclei lysis buffer *( )*. Chromatin was diluted in 500 µl of ChIP dilution buffer [1% Triton X-100 (Santa Cruz Biotech), 2 mM EDTA, 150 mM NaCl (Sigma), 20 mM Tris-HCl, pH 8.0] and split into 1.5 ml microcentrifuge tubes, 300 µl per tube. Chromatin was sonicated using the Qsonica Q700A Sonicator with a 5.5 in Cup Horn, spun for 10 min at 4 °C at 1×10^4 g, and efficiency was confirmed using the Agilent 2200 Tapestation. Sonicated chromatin from 5×10^6 cells was diluted in 1.5 ml siliconized, low-binding tubes (Sigma) in ChIP dilution buffer to 1 ml for each pulldown, except for the p65 sorted experiments where chromatin from 1.5×10^6 cells was used. Chromatin was precleared by incubation with 20 µl of Magna ChIP Protein A + G beads (Millipore) (washed 3 times with 5 mg/ml BSA (Sigma) in 1× PBS) for 3 h at 4 °C with nutation. Beads were separated and removed using a magnetic rack (Invitrogen), 50 µl from each chromatin prep was frozen for inputs, and chromatin was incubated with antibody [5 µl anti-Histone H3 antibody (ab1791, Abcam); 5 µl anti-H3K27me3 antibody (07−449, Millipore); 3 µl anti-H3K4me3 (ab8580, Abcam)] for 12 h at 4 °C with nutation. Chromatin was incubated with 20 µl washed Magna ChIP beads for 3 h at 4 °C with nutation. Beads were washed at 4 °C 3 times, first with 1 ml low salt buffer [20 mM Tris-HCl, 2 mM EDTA, 1% Triton X-100, 0.1% SDS (Sigma), 150 mM NaCl (Sigma)], 1 ml high salt buffer [20 mM Tris-HCl, 2 mM EDTA, 1% Triton X-100, 0.1% SDS, 500 mM NaCl], and 1 ml tris-EDTA pH 7.6 (Sigma) with 10 min incubations with nutation between each wash. Beads were resuspended in 100 µl elution buffer [1% SDS, 0.1 M $NaHCO_3$ (Sigma), 0.1 M NaCl], inputs were thawed and diluted with 50 µl elution buffer, and all samples were incubated for 30 min at room temperature with nutation. Samples were incubated at 65 °C for 7 h for uncrosslinking, at 45 °C for 14 h with 20 µg of Proteinase K (Thermo-Fisher), and eluted in 50 µl nuclease-free water using the Genelute PCR Cleanup Kit (Sigma).

4.6 Quantitative PCR of ChIP DNA

Relative quantification of ChIP samples was performed using real-time quantitative PCR and SYBR Green I master mix (Roche) as previously described.[10] To adjust for input dilution, $\log_2 20$ was subtracted from input Cp values.

% IP DNA bound was calculated as $100 \times 2^{\text{Ct input–Ct IP}}$. % IgG-IP bound ($100 \times 2^{\text{Ct input–Ct IgGIP}}$) was subtracted from % IP DNA bound to calculate % IP enrichment for H3K27me3 and H3K4me3 ChIP samples. Primer sequences for *luciferase* and TBP are listed in Supplementary Table S5.

4.7 Statistical Analyses

The percentage of edited reads was normalized to transfection efficiency for each sample. Averages and standard deviations were calculated for each of $n = 3$ biological replicates.

To analyze ChIP-qPCR assay data, averages and standard deviations were calculated for each of $n = 3$ replicate IPs from a single chromatin preparation. For each cell/treatment data set, percent IP DNA for site 1 and TBP were normalized to

percent IP DNA for TBP.

The differences of means to compare cell/treatment data sets for both editing and ChIP-qPCR experiments were calculated using the two sample, one-tailed Student's t test. For $p < 0.05$, 95% confidence with 2 degrees of freedom and a test statistic of $t_{(0.05,2)} = 2.920$. For $p < 0.01$, 99% confidence with 2 degrees of freedom and a test statistic of $t_{(0.01,2)} = 6.965$.

5 Acknowledgments

This work was supported by NSF CBET (1404084). RMD was supported by the ARCS Foundation. KAH was supported by NIH NCI (K01 CA188164). The authors thank the Center for Computational and Integrative Biology (CCIB) Core Facility (Massachusetts General Hospital, Cambridge, MA) for providing CRISPR sequencing services. TBP primers were a generous gift from J. Cutts (Brafman Lab at ASU, Tempe, AZ) and the Luc14 and GAL4EED cell lines were a generous gift from K. Hansen. The authors thank J. Daer for critical review of this manuscript.

References

(*1*) Jinek, M., Chylinski, K., Fonfara, I., Hauer, M., Doudna, J. a., and Charpentier, E., (Aug. 2012). A Programmable Dual-RNA-Guided DNA Endonuclease in Adaptive Bacterial Immunity. *Science 337*, 816–821, DOI: 10.1126/science.1225829.

(*2*) Gilbert, L. A., Larson, M. H., Morsut, L., Liu, Z., Brar, G. A., Torres, S. E., Stern-Ginossar, N., Brandman, O., Whitehead, E. H., Doudna, J. A., Lim, W. A., Weissman, J. S., and Qi, L. S., (July 2013). CRISPR-Mediated Modular RNA-Guided Regulation of Transcription in Eukaryotes. *Cell 154*, 442–451, DOI: 10.1016/j.cell.2013.06.044.

(*3*) Tiwari, V. K., Cope, L., McGarvey, K. M., Ohm, J. E., and Baylin, S. B., (2008). A novel 6C assay uncovers Polycomb-mediated higher order chromatin conformations. *Genome Research 18*, 1171–1179, DOI: 10.1101/gr.073452.107.

(*4*) Bell, O., Tiwari, V. K., Thomä, N. H., and Schübeler, D., (2011). Determinants and dynamics of genome accessibility. *Nature Reviews Genetics 12*, 554–564, DOI: 10.1038/nrg3017.

(*5*) Aoto, T., Saitoh, N., Sakamoto, Y., Watanabe, S., and Nakao, M., (July 2008). Polycomb group protein-associated chromatin is reproduced in post-mitotic G 1 phase and is required for S phase progression. *Journal of Biological Chemistry 283*, 18905–18915, DOI: 10.1074/jbc.M709322200.

(*6*) Hinz, J. M., Laughery, M. F., and Wyrick, J. J., (2015). Nucleosomes Inhibit Cas9 Endonuclease Activity in Vitro. *Biochemistry 54*, 7063–7066, DOI: 10.1021/acs.biochem.5b01108.

(*7*) Isaac, R. S., Jiang, F., Doudna, J. A., Lim, W. A., Narlikar, G. J., and Almeida, R., (Apr. 2016). Nucleosome breathing and remodeling constrain CRISPR-Cas9 function. *eLife 5*, 1–14, DOI: 10.7554/eLife.13450.

(*8*) Horlbeck, M. A., Witkowsky, L. B., Guglielmi, B., Replogle, J. M., Gilbert, L. A., Villalta, J. E., Torigoe, S. E., Tjian, R., and Weissman, J. S., (2016). Nucleosomes impede cas9 access to DNA in vivo and in vitro. *eLife 5*, 1–21, DOI: 10.7554/eLife.12677.

(*9*) Chen, X., Rinsma, M., Janssen, J. M., Liu, J., Maggio, I., and Gonçalves, M. A., (2016). Probing the impact of chromatin conformation on genome editing tools. *Nucleic Acids Research 44*, 6482–6492, DOI: 10.1093/nar/gkw524.

(*10*) Daer, R. M., Cutts, J. P., Brafman, D. A., and Haynes, K. A., (Mar. 2017). The Impact of Chromatin Dynamics on Cas9-Mediated Genome Editing in Human Cells. *ACS Synthetic Biology 6*, 428–438, DOI: 10.1021/acssynbio.5b00299.

(*11*) Anderson, J., and Widom, J., (Mar. 2000). Sequence and position-dependence of the equilibrium accessibility of nucleosomal DNA target sites 1 1Edited by T. Richmond. *Journal of Molecular Biology 296*, 979–987, DOI: 10.1006/jmbi.2000.3531.

(*12*) Partensky, P. D., and Narlikar, G. J., (Aug. 2009). Chromatin Remodelers Act Globally, Sequence Positions Nucleosomes Locally. *Journal of Molecular Biology 391*, 12–25, DOI: 10.1016/j.jmb.2009.04.085.

(*13*) Racey, L. A., and Byvoet, P., (1971). Histone acetyltransferase in chromatin. Evidence for in vitro enzymatic transfer of acetate from acetyl-coenzyme A to histones. *Experimental Cell Research 64*, 366–370, DOI: 10.1016/0014-4827(71)90089-9.

(*14*) Rea, S., Eisenhaber, F., O'Carroll, D., Strahl, B. D., Sun, Z. W., Schmid, M., Opravil, S., Mechtler, K., Ponting, C. P., Allis, C. D., and Jenuwein, T., (2000). Regulation of chromatin structure by site-specific histone H3 methyltransferases. *Nature 406*, 593–599, DOI: 10.1038/35020506.

(*15*) Konze, K. D., Ma, A., Li, F., Barsyte-Lovejoy, D., Parton, T., MacNevin, C. J., Liu, F., Gao, C., Huang, X.-p., Kuznetsova, E., Rougie, M., Jiang, A., Pattenden, S. G., Norris, J. L., James, L. I., Roth, B. L., Brown, P. J., Frye, S. V., Arrowsmith, C. H., Hahn, K. M., Wang, G. G., Vedadi, M., and Jin, J., (June 2013). An Orally Bioavailable Chemical Probe of the Lysine Methyltransferases EZH2 and EZH1. *ACS Chemical Biology 8*, 1324–1334, DOI: 10.1021/cb400133j.

(*16*) Polstein, L. R., Perez-pinera, P., Kocak, D. D., Vockley, M., Bledsoe, P., Song, L., Safi, A., Crawford, G. E., Reddy, T. E., Gersbach, C. a., Carolina, N., and Surgery, O., (2015). Genome-wide specificity of DNA binding , gene regulation , and chromatin remodeling by TALE- and CRISPR / Cas9-based transcriptional activators. *Genome research 25*, 1158–1169, DOI: 10.1101/gr.179044.114..

(*17*) Morey, L., Pascual, G., Cozzuto, L., Roma, G., Wutz, A., Benitah, S. A., and Di Croce, L., (Jan. 2012). Nonoverlapping functions of the Polycomb group Cbx family of proteins in embryonic stem cells. *Cell Stem Cell 10*, 47–62, DOI: 10.1016/j.stem.2011.12.006.

(*18*) Morey, L., Santanach, A., Blanco, E., Aloia, L., Nora, E. P., Bruneau, B. G., and Di Croce, L., (Sept. 2015). Polycomb regulates mesoderm cell fate-specification in embryonic stem cells through activation and repression mechanisms. *Cell Stem Cell 17*, 300–315, DOI: 10.1016/j.stem.2015.08.009.

(*19*) van Lohuizen, M., Frasch, M., Wientjens, E., and Berns, A., (Sept. 1991). Sequence similarity between the mammalian bmi-1 proto-oncogene and the Drosophila regulatory genes Psc and Su(z)2. *Nature 353*, 353–355, DOI: 10.1038/353353a0.

(*20*) Jacobs, J. L., Scheijen, B., Voncken, J. W., Kieboom, K., Berns, A., and van Lohuizen, M., (1999). Bmi-1 collaborates with c-Mycin tumorigenesis by inhibiting c-Myc-induced apoptosis via INK4a/ARF. *Genes {&} Development*, 2678–2690, DOI: 10.1101/gad.13.20.2678.

(*21*) Jacobs, J. J., Kieboom, K., Marino, S., DePinho, R. A., and van Lohuizen, M., (Jan. 1999). The oncogene and Polycomb-group gene bmi-1 regulates cell proliferation and senescence through the ink4a locus. *Nature 397*, 164–168, DOI: 10.1038/16476.

(*22*) Schuettengruber, B., Bourbon, H. M., Di Croce, L., and Cavalli, G., (2017). Genome regulation by Polycomb and Trithorax: 70 years and counting. *Cell 171*, 34–57, DOI: 10.1016/j.cell.2017.08.002.

(*23*) Hansen, K. H., Bracken, A. P., Pasini, D., Dietrich, N., Gehani, S. S., Monrad, A., Rappsilber, J., Lerdrup, M., and Helin, K., (Nov. 2008). A model for transmission of the H3K27me3 epigenetic mark. *Nature Cell Biology 10*, 1291–1300, DOI: 10.1038/ncb1787.

(*24*) Lee, M. G., Villa, R., Trojer, P., Norman, J., Yan, K.-P., Reinberg, D., Croce, L. D., and Shiekhattar, R., (2007). Demethylation of H3K27 regulates Polycomb recruitment and H2A ubiquitination. *Science 318*, 447–450, DOI: 10.1126/science.1149042.

(*25*) McGarvey, K. M., Greene, E., Fahrner, J. A., Jenuwein, T., and Baylin, S. B., (June 2007). DNA Methylation and Complete Transcriptional Silencing of Cancer Genes Persist after Depletion of EZH2. *Cancer Research 67*, 5097–5102, DOI: 10.1158/0008-5472.CAN-06-2029.

(*26*) Szklarczyk, D., Franceschini, A., Wyder, S., Forslund, K., Heller, D., Huerta-Cepas, J., Simonovic, M., Roth, A., Santos, A., Tsafou, K. P., Kuhn, M., Bork, P., Jensen, L. J., and von Mering, C., (Jan. 2015). STRING v10: protein–protein interaction networks, integrated over the tree of life. *Nucleic Acids Research 43*, D447–D452, DOI: 10.1093/nar/gku1003.

(*27*) Ea, C.-K., and Baltimore, D., (Nov. 2009). Regulation of NF-KB activity through lysine monomethylation of p65. *Proceedings of the National Academy of Sciences 106*, 18972–18977, DOI: 10.1073/pnas.0910439106.

(*28*) Bernstein, B. E., Mikkelsen, T. S., Xie, X., Kamal, M., Huebert, D. J., Cuff, J., Fry, B., Meissner, A., Wernig, M., Plath, K., Jaenisch, R., Wagschal, A., Feil, R., Schreiber, S. L., and Lander, E. S., (Apr. 2006). A bivalent chromatin structure marks key developmental genes in embryonic stem cells. *Cell 125*, 315–26, DOI: 10.1016/j.cell.2006.02.041.

Supplementary

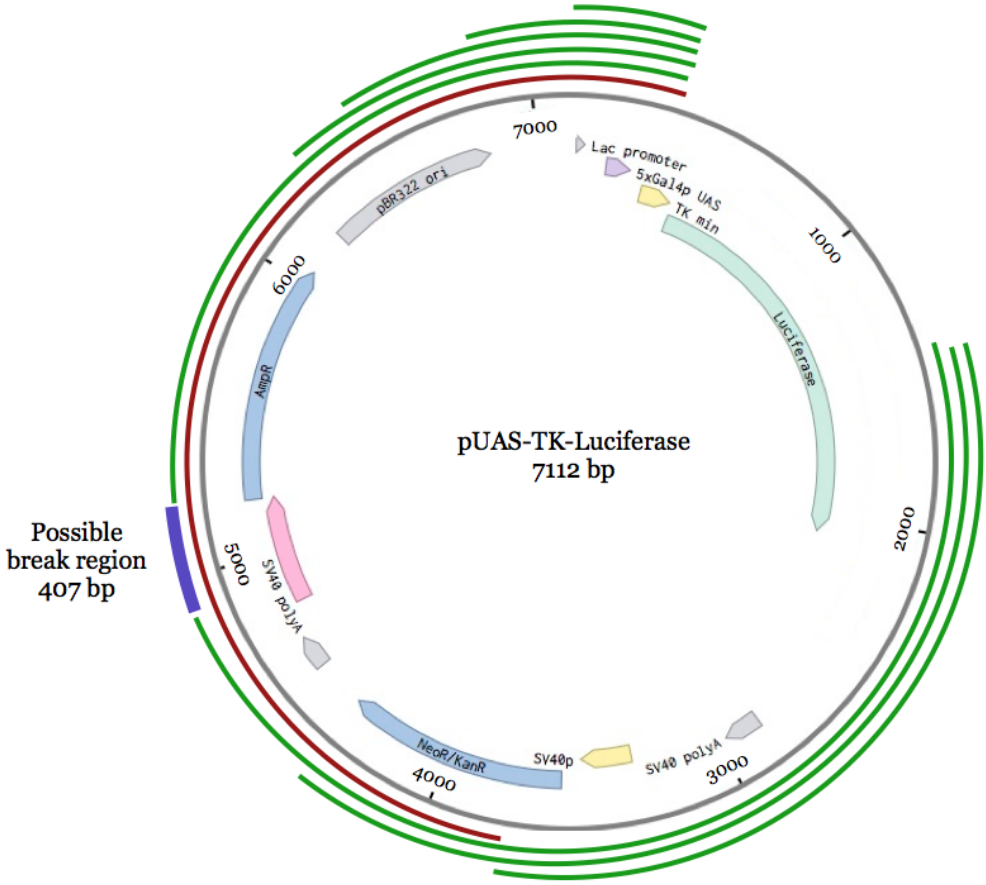

Figure S1: PCR analysis of *pUAS-TK-Luciferase* Transgene Map. PCR analysis was performed to identify the region that includes the plasmid break point before genomic insertion during cell line generation. Map of the *pUAS-TK-luciferase* transgene (generated by Benchling software) includes plasmid and gene annotations a well as successful (green curves) PCR amplicons and unsuccessful expected amplicons (red curves). The purple curve annotates the 407 basepair region predicted to include the plasmid break point. Each amplification included an anchor primer in the transgene sequence as there are several transgenes in this cell line and plasmid sequences may not be unique. Importantly, single integration was not confirmed for this transgene.

Table S1: UNC1999 Kill Curve. Toxicity was determined by estimating via microscopy adherent confluency compared to a vehicle control (DMSO-treated) well.

Concentration (μM)	Toxicity
0 vehicle	None
1	None
2	None
5	None
10	None
20	Some
50	Toxic

Table S2: List of Primers for PCR of Genomic DNA from Cas9/sgRNA Treated Samples

Forward Primer		Reverse Primer	
Name	Sequence	Name	Sequence
P197	5'–CTCACTCATTAGGCACCCC–3'	P198	5'–CGTTGGTCGCTTCCGGAT–3'

Table S3: List of Primers for Nested PCR of Genomic DNA from Cas9/sgRNA Treated Samples

gRNA	RNA Site	Forward Primer	Reverse Primer
g046	5'–CCTGCATAAGCTTGCCA | CCA tgg–3'	P355	P311
g032	5'–CCTCTAGAGGATGGAAC | CGC tgg–3'	P163	P348
g025	5'–cct ACC | GTAGTGTTTGTTTCCAA–3' 3'–TTGGAAACAAACACTAC | GGT agg–5'	P332	P330
g048	5'–GGATCTACTGGGTTACC | TAA ggg–3'	P314	P318

Table S4: Sequences for Primers for Nested PCR of Genomic DNA from Cas9/sgRNA Treated Samples

Primer Name	Sequence
P163	5'–CAAACCCCGCCCAGCGTCTTA–3'
P311	5'–CCGCGTACGTGATGTTCACC–3'
P314	5'–CGTTCGTCACATCTCATCTACC–3'
P318	5'–TCCGGAATGATTTGATTGCC–3'
P330	5'–TAGATGAGATGTGACGAACGTG–3'
P332	5'–CGCCCGCGAACGACATTTATAATG–3'
P348	5'–TTGTTCCAGGAACCAGGGCG–3'
P355	5'–TCCGAGGTCCACTTCGCATA–3'

Table S5: List of Primers for ChIP-qPCR

	Forward Primer		Reverse Primer	
qPCR Target Site	Name	Sequence	Name	Sequence
Luciferase	P360	5'–CGGCGCCATTCTATCCTCTA–3'	P361	ATTCCGCGTACGTGATGTTC–3'
TBP	P363	CAGGGGTTCAGTGAGGTCG–3'	P364	CCCTGGGTCACTGCAAAGAT–3'